

Structure and electronic properties of hydrogenated amorphous silicon nitride from first-principles

K. Jarolimek^{*†‡}, R. A. de Groot[†], G. A. de Wijs[†] and M. Zeman^{*}

^{*} Delft University of Technology, DIMES

Feldmannweg 17, 2600 GB Delft, The Netherlands

[†] Electronic Structure of Materials, Institute for Molecules and Materials

Radboud University Nijmegen, Heyendaalseweg 135, 6525 AJ Nijmegen, The Netherlands

[‡] Email: k.jarolimek@science.ru.nl

Abstract—Our research is aimed at multilayers of hydrogenated amorphous silicon (a-Si:H) and hydrogenated amorphous silicon nitride (a-SiN_x:H). We are particularly interested in the interface between these two materials that are formed in multilayered structures. These structures can be used as selective absorbers of light in a new generation of thin film solar cells [1]. The multilayer can be tuned to absorb visible light of certain wavelength by modifying the concentration of nitrogen in a-SiN_x:H. Having completed our studies on a-Si:H we focus on the silicon nitride. Our approach is based on a molecular dynamics simulation within the Density Functional Theory approximation. This method is referred to as *ab initio* i.e. it requires no input from experiment. The procedure consists of heating a random configuration of silicon, nitrogen and hydrogen atoms to 3060 K, forming a liquid and subsequently cooling it down to room temperature. We make use of several cooling rates to estimate their effect on the quality of the amorphous structure. We find a noticeable improvement with slower cooling demonstrated by changes in structural properties e.g. partial radial distributions and bond angle distributions. Further, we calculate the electronic density of states and obtain a band gap with several in-gap states. In some cases in-gap states can be related to structural defects such as under-coordinated or over-coordinated atoms or "wrong" silicon-silicon bonds. This study tries to answer fundamental questions on the geometric structure of a-SiN_x:H, the local atomic arrangement of defects and their coupling to electronic defect states inside the gap. The results may help in better understanding of a relatively unexplored material and in the interpretation of experimental data.

I. INTRODUCTION

Amorphous silicon nitride is a material of considerable technological interest. It is used as insulator in integrated circuits technology [2]. Silicon nitride films have excellent diffusion limiting properties and can be utilized as masks for semiconductors to protect against donor and acceptor impurity diffusion [3]. a-SiN_x is chemically stable and can withstand corrosive action of most reagents. Other applications include anti-reflection coatings in solar cells and optical waveguides.

Thin films of silicon nitride are deposited using various techniques e.g. chemical vapor deposition (CVD), plasma deposition (PECVD) and sputtering. The composition of the material is non-stoichiometric in general and contains varying amounts of hydrogen depending on the preparation conditions.

Along with the experimental interest in a-SiN_x, several theoretical studies were performed. First a realistic structural model of the amorphous network needed to be obtained.

Samples of a-SiN_x were mostly prepared by a "cooling from liquid" approach, where a liquid alloy of silicon and nitrogen is cooled to room temperature using molecular dynamics simulation. Another approach is to perform simulated annealing using Monte Carlo simulations. In both cases, the system ends up in a metastable (amorphous) state. The accuracy of such simulations ranges from classical, model potential [4], [5], [6], [7], [8], [9] to *ab initio* [10], [11]. Since classical simulations are less demanding in terms of computer power, larger systems with medium range order can be studied such as nanophase silicon nitride [12], [13], [14], [15].

Note that most of the studies listed above combine the classical and *ab initio* methods. The amorphous samples are prepared by classical molecular dynamics or Monte Carlo simulation. Then the electronic structure of the resulting structure is calculated using a suitable *ab initio* method. Kroll [16] extended the WWW bond switching algorithm [17] to generate samples of a-SiN_x. Alvarez et. al used *ab initio* MD to prepare a series of samples of a-SiN_x with different compositions. A convenient approach to study the electronic structure of amorphous solids is to use a Bethe lattice as a model. Several studies that use a tight binding Hamiltonian were performed [18], [19], [20], [21], [22], [23]. All of the studies listed above are on pure silicon nitride, except a classical MD study by Justo et. al [9], Bethe lattice studies by Lin et. al [18], [19] and a Hartree-Fock cluster study by Ordejon et. al [10].

Our long term research aims are multilayers of a-Si:H and a-SiN_x:H. The multilayer structure is grown by the PECVD process and thus both layer materials contain considerable amounts of hydrogen. a-SiN:H that was used to deposit the multilayers has a nitrogen over silicon ratio of approximately one and a optical band gap of 2.85 eV [1]. The concentration of nitrogen in turn has influence on the hydrogen concentration and results in a Si_{0.34}N₃₅H₃₁ composition. The width of the nitride layer can be tuned to obtain a desired effective band gap of the multilayer. This has promising applications in tandem thin film solar cells that utilize the solar spectrum in a better way.

II. TECHNICAL DETAILS

We use a first principles MD to prepare models of a-SiN_x:H. The term “first principles” denotes that there is no experimental input to the calculations. First principles MD are more accurate than classical MD, since the interaction between atoms is treated quantum mechanically. The diverse chemical reactions (the forming and breaking of bonds) can be actually observed during the quench. On the other hand first principles MD are much more computationally demanding and thus are limited to shorter simulation times.

The total energy and forces are calculated within the Density Functional Theory (DFT) using a Generalized Gradient Approximation (GGA) [24]. We use the Vienna *Ab initio* Simulation Package (VASP) [25], [26]. Electron-ion interactions are described using the projector augmented wave method [27], [28]. The kinetic energy cutoff is set to 300 eV. During the whole MD run and the relaxation, we use only the Γ point for Brillouin zone sampling. The partial occupancies are determined by the Methfessel-Paxton method [29] with a smearing width of 0.2 eV. For calculations on the relaxed structures we use a $5 \times 5 \times 5$ Monkhorst-Pack mesh [30] for the Brillouin Zone sampling and a Gaussian broadening of 0.05 eV.

The highest vibrational frequency which can occur during the simulation is due to the vibration of the hydrogen molecule. The silicon-hydrogen stretching mode has the second highest frequency. We set our time step to 1 fs which proves to be sufficient to describe the latter case. The integration of the vibrational motion of the hydrogen molecule using this time step is rather crude. However the time step of 1 fs is a reasonable compromise between computational cost and accuracy.

III. PREPARATION OF THE STRUCTURE

The amorphous structures are prepared by a cooling from a liquid approach. At first atoms are placed randomly in the supercell so that the distances between them are larger than the sum of their covalent radii. This prevents the building of large forces in the beginning of the molecular dynamics. The velocities of the atoms are initialized according to the Maxwell-Boltzmann distribution such that the temperature of the system is 300 K. Next the system is heated to 3060 K with a constant rate of 1.38 K/fs. At this temperature the system is a liquid, with the root mean squared displacement growing linearly in time. The density of states has a depression around the Fermi energy, however no band gap is formed. The liquid is equilibrated for 8 ps at this temperature. Next the sample is cooled back to room temperature. We utilize three different cooling rates 1.380 K/fs, 0.138 K/fs and 0.023 K/fs (see Fig. 1). We will refer to them as fast, normal and slow cooling rate. After reaching 300 K the samples are evolved for another 0.5 ps to calculate the structural averages.

IV. SAMPLES PREPARED BY SLOW COOLING

A convenient way to describe disordered systems is the radial distribution function $g(r)$. It gives a probability of

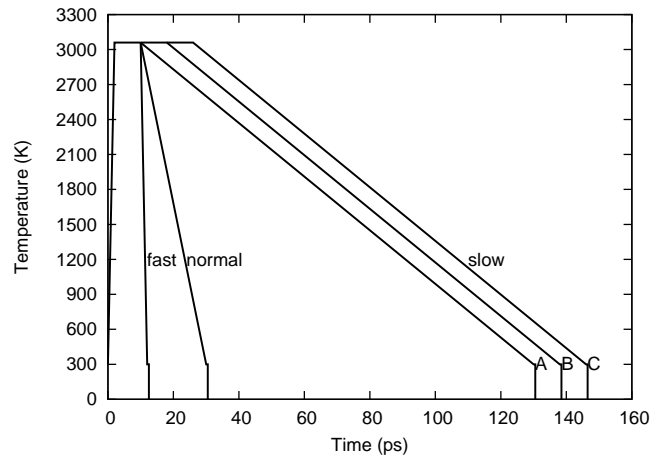


Fig. 1. Thermal procedure used to prepare amorphous structures of a-SiN_x:H. The three slow quench samples are marked with letters A, B and C.

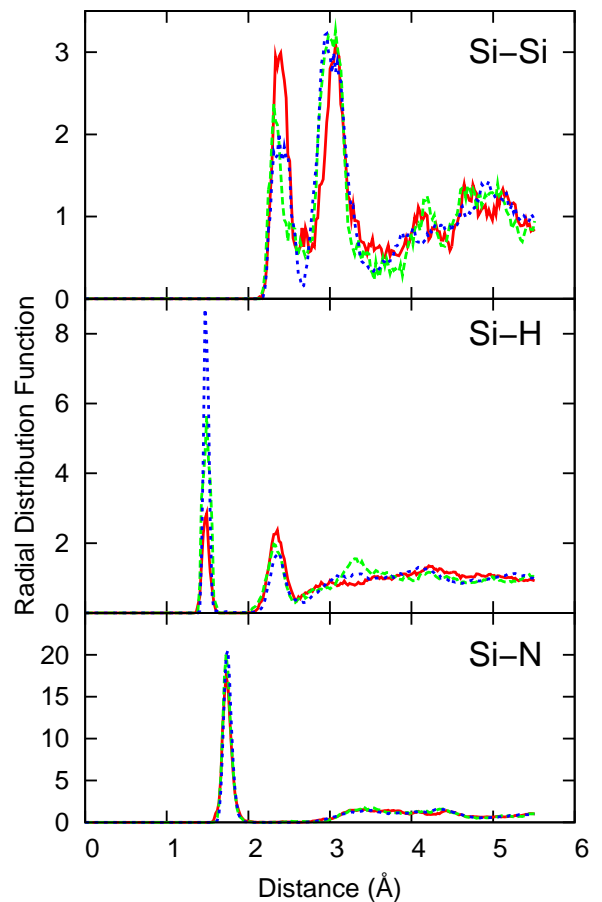


Fig. 2. Partial radial distributions: Si-Si (upper part), Si-H (middle part) and Si-N (lower part) as prepared by fast (solid red line), normal (dashed green line) and slow (dotted blue line) rate. The distributions refer to systems at 300 K.

finding two atoms at a distance r apart. Since our system comprises three different elements there is a total of six partial distributions (see Figs. 2, 3). The Si-Si radial distribution has

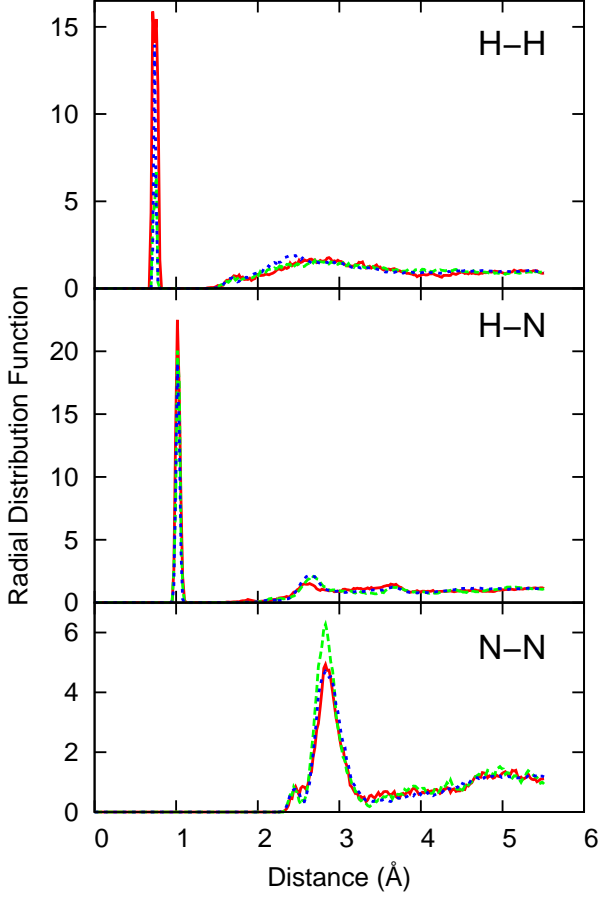


Fig. 3. Partial radial distributions: H-H (upper part), H-N (middle part) and N-N (lower part) as prepared by fast (solid red line), normal (dashed green line) and slow (dotted blue line) rate. The distributions refer to systems at 300 K.

two prominent peaks. The first peak is due to Si-Si bonds and due to silicon atoms that form square shaped structures. The “square structures” are formed by two silicon atoms in opposite corners along with two nitrogen atoms placed in the remaining corners. The structure is planar with angles close to 90° . The second peak is formed by silicon atoms that are connected to a common nitrogen atom. The Si-H and H-N radial distributions have well defined and sharp first peaks that are due to hydrogen atom bonded to silicon or nitrogen atoms respectively. The peak positions in g_{Si-H} and g_{H-N} correspond to calculated bond lengths in the SiH_4 and NH_3 molecules respectively. The static deviation (deviation at 0 K) of the Si-N bond length is found to be relatively small compared to Si-Si bonds. Hydrogen molecules are formed in all of the samples as can be seen from the peak at 0.7 \AA in the H-H partial distribution. Similarly to the g_{Si-Si} function, the N-N distribution contains two peaks. The first peak is due to nitrogen atoms that form the “square structures”. The second, more intensive peak, is due to nitrogen atoms bonded to a common silicon atom. Note that there are no N-N bonds present in the samples and thus the corresponding

TABLE I
STRUCTURAL PARAMETERS OF SAMPLES PREPARED BY SLOW COOLING. THE AVERAGE ATOMIC DISTANCES r ARE CALCULATED AT 300 K. THE DEVIATIONS σ REFER TO STATIC DISORDER ONLY, AND ARE CALCULATED AT 0 K.

sample	r_{Si-Si}^1	r_{Si-Si}^2	r_{Si-N}^1	r_{N-N}^1	r_{N-N}^2
A	2.45	3.09	1.77	2.44	2.92
B	2.42	3.09	1.76	2.46	2.92
C	2.42	3.04	1.76	2.48	2.93
aver.	2.43	3.07	1.76	2.46	2.92
	σ_{Si-Si}^1	σ_{Si-Si}^2	σ_{Si-N}^1	σ_{N-N}^1	σ_{N-N}^2
A	0.097	0.177	0.033	0.039	0.144
B	0.089	0.168	0.029	0.038	0.142
C	0.066	0.145	0.032	0.045	0.150
aver.	0.087	0.166	0.032	0.047	0.146

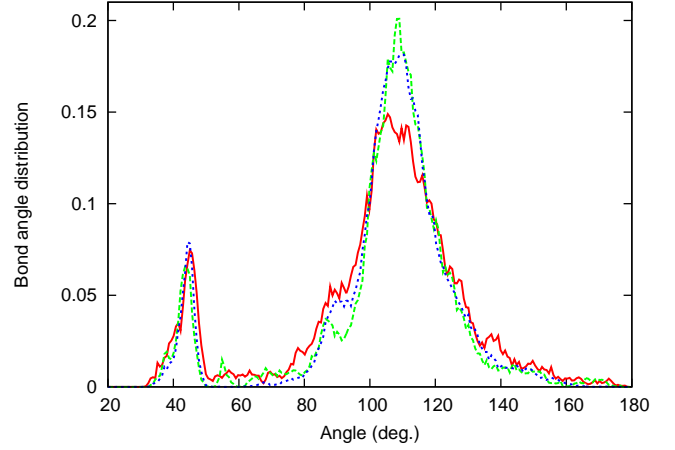


Fig. 4. Distribution of bond angles centered on silicon atoms (solid red line) and nitrogen atoms (dashed green line). The distributions are averages over three samples prepared by slow cooling and refer to systems at 300 K.

peak is missing. The peak positions and static deviations are summarized in Table I. The presence of the “square structures” is also indicated by the bond angle distributions (see Fig. 4). We will denote the angles centered on silicon and nitrogen atoms as θ_{Si} and θ_N respectively. The distribution of θ_{Si} can be divided roughly into two contributions. The contribution of the tetrahedral network (peak at $\sim 109^\circ$) and a contribution of the square structures (peaks at $\sim 45^\circ$ and $\sim 90^\circ$). The situation is analogical in the θ_N distribution. The peak at $\sim 90^\circ$ is due to nitrogen atoms that form square structures. The second peak at $\sim 120^\circ$ arises from nitrogen atoms bonded to three silicon atoms in a planar configuration. Thus the structure of a-SiN:H can be viewed as a heavily distorted network of crystalline Si_3N_4 (either α or β phase) penetrated with “square structures”. The peak positions and deviations of the particular peaks that contribute to the overall angle distributions are summarized in Table II.

V. STRUCTURAL AND ELECTRONIC DEFECTS

To evaluate the number of structural defects one first needs to set up a criterion that identifies bonded atoms. The obvious thing to do is to define six cut-off distances. If the distance between two atoms is smaller than the particular cut-off distance

TABLE II

POSITIONS OF THE PEAKS CONTRIBUTING TO THE TOTAL BOND ANGLE DISTRIBUTIONS CENTERED ON SI AND N ATOMS. ALL VALUES REFER TO SYSTEMS AT 0 K.

sample	θ_{Si}^{45}	θ_{Si}^{90}	θ_{Si}^{109}	θ_N^{90}	θ_N^{120}
A	43.47	86.92	111.08	93.05	119.65
B	44.85	88.66	111.83	90.31	120.39
C	45.37	89.67	112.26	89.26	118.98
aver.	44.69	88.60	111.73	90.62	119.68

TABLE III

THE POSITION OF THE FIRST AND SECOND MINIMUM IN THE SIX PARTIAL RADIAL DISTRIBUTIONS. THE POSITION OF THE FIRST MINIMUM IS USED AS A CUT-OFF DISTANCE (EXCEPT FOR N-N BONDS). ALL DISTANCES ARE IN ÅNGSTRÖM.

	Si-Si	Si-H	Si-N	H-H	H-N	N-N
cut-off	2.65	1.79	2.16	0.90	1.18	1.20
1st minimum	2.65	1.79	2.16	0.90	1.18	2.56
2nd minimum	3.53	-	-	-	-	3.36

TABLE IV

NUMBER OF DEFECTS PRESENT IN THE SAMPLES PREPARED BY SLOW COOLING. THE UPPER PART OF THE TABLE GIVES THE NUMBER OF DEFECTS USING SOLELY THE CUT-OFF DISTANCE CRITERION. THE LOWER PART TAKES THE DIRECTIONALITY OF THE BONDS INTO ACCOUNT. THE NUMBER OF "SQUARE STRUCTURES" IS DENOTED "S", THE NUMBER OF SI-SI BONDS AS " B_{Si-Si} ".

sample	Si3	Si5	Si6	N2	N4	S	B_{Si-Si}
A	-	8	-	1	1	4	21
B	-	8	1	-	-	5	22
C	1	10	1	1	-	6	21
A	-	-	-	1	1	4	17
B	-	-	-	-	-	5	17
C	1	-	-	1	-	6	15

they are considered to be bonded. The cut-off distances are chosen as a minimum after the first peak in the corresponding partial radial distribution. The exception to this rule is the N-N bond, since there are no such bonds present in our samples. The N-N cut-off distance is set approximately to the bond length of the N_2 molecule. The various cut-off distances are summarized in Table III. After specifying the cut-off distances one can calculate the number of defects and coordination numbers. By defects we mean silicon atoms that are other than 4-fold coordinated and nitrogen atoms that are not 3-fold coordinated. It turns out, however, that the cut-off criterion is rather simplistic. The bonds that are formed by silicon and nitrogen atoms have a strongly directional character. That means that two atoms can be closer than the particular cut-off distance but they are not bonded. This occurs in the "square structures" where the two silicon atoms are within the cut-off distance but they are not bonded to each other. It is rather clear that one arrives to different counts of defects and coordination numbers depending on which criterion is applied. The upper part of Table IV gives the number of defects using the cut-off distance criterion, the lower part of the table takes also the directionality of the bonds into account. Depending on the criterion chosen one also arrives at different coordination numbers (see Tab. V). In fact the upper part of

TABLE V

COORDINATION NUMBERS OF SI AND N ATOMS IN SAMPLES PREPARED BY SLOW COOLING. THE VALUES IN THE UPPER PART OF THE TABLE ARE OBTAINED BY THE CUT-OFF CRITERION. THE LOWER PART TAKES THE DIRECTIONAL BONDING INTO ACCOUNT.

sample	Si	N
A	4.21	3.00
B	4.26	3.00
C	4.29	2.97
A	4.00	3.00
B	4.00	3.00
C	3.97	2.97

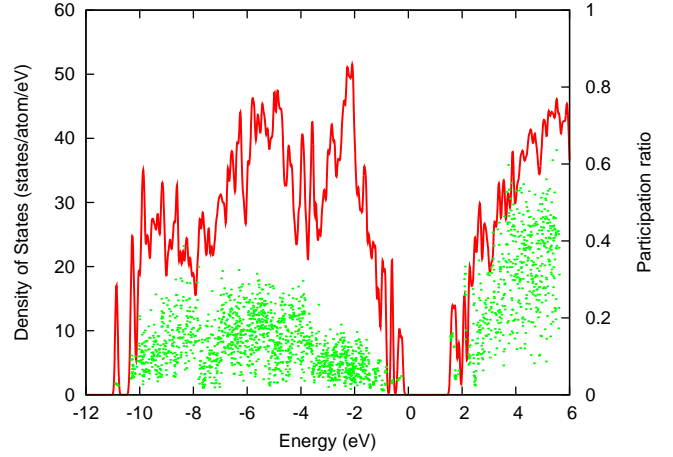


Fig. 5. Calculated electronic density of states (red line) and participation ratio (green dots) of sample A.

the table would not change if one integrates the first peak of the particular partial radial distribution. However, taking the directionality of the bonds into account we can see that the Si and N atoms are on average close to coordination number of 4 and 3 respectively. Note that the sample A has Si and N coordination of 4 and 3 respectively. This doesn't mean that the sample is defect free, in this case the effect of under/over-coordination evens out. It is difficult to draw any conclusions on the concentration of defects present in a-SiN_x:H due to limited statistics.

In Figure 5 we give the calculated density of states of the sample A along with the participation ratio for each distinct electronic state. The participation ratio p_i is a measure of localization. It is calculated by projecting the wave function ψ_i onto spherical harmonics, which are non-zero only in spheres centered on each atom j . The participation ratio is defined as follows (see, e.g. [31]):

$$p_i = \left(\sum_{j=1}^N \sum_{l=1}^3 c_l^2(\vec{R}_j) \right)^2 \left(N \sum_{j=1}^N \sum_{l=1}^3 c_l^4(\vec{R}_j) \right)^{-1}.$$

The sums run over angular-momentum components l and over each atom with coordinates \vec{R}_j . The order of the spherical harmonics function m is already absorbed in the expansion coefficients c_l . The ratio approaches N^{-1} , where N is the number of atoms in the supercell, for a maximally localized

TABLE VI

STRUCTURAL DEFECTS IN SAMPLES PREPARED BY DIFFERENT COOLING RATES. THE DIRECTIONAL CHARACTER OF BONDING IS TAKEN INTO ACCOUNT. THE SYMBOL “S” DENOTES THE NUMBER OF “SQUARE STRUCTURE”. “ B_{Si-Si} ” DENOTES THE NUMBER OF SI-SI BONDS.

rate	Si3	Si5	Si6	N2	N4	S	B_{Si-Si}	H2
fast	5	–	–	2	1	6	22	4
normal	4	–	–	1	1	4	16	1
slow (aver.)	0.3	–	–	0.7	0.3	5	16.3	1.3

state. A delocalized state, e.g. a plane wave, has a participation ratio of 1.

With the help of the participation ratio it is possible to discriminate between defect states (inside the band gap) and band edge states (at least qualitatively), since defect states are more localized. Most of the electronic defects can be coupled to structural defects in the samples. The 2-fold coordinated nitrogen atom in sample A contributes to several defect states near the valence band edge. The 4-fold coordinated nitrogen atom induces a defect state near the conduction band edge. Sample B has no structural defects and this is in agreement with the electronic point of view. Similarly to sample A, sample C has a 2-fold coordinated nitrogen atom, giving rise to a state near the valence band. A second defect, in sample C, is a 3-fold coordinated Si atom inducing a state near the conduction band. In addition to the defect states, we find that Si-Si bonds give rise to states near the band gap edges. This is in agreement with measurements of the optical gap with varying composition of a-SiN_x:H. The band gap value increases with increasing nitrogen content or decreasing number of Si-Si bonds. Interestingly, nitrogen atoms that are 3-fold coordinated do contribute to defect states, but only near the valence band. These states have a π like character. The average band gap is 2.42 eV with a deviation of 0.14 eV. It has to be noted that the DFT approximation underestimates semiconductor band gap values in general.

VI. EFFECT OF THE COOLING RATE

The preparation of models of amorphous solids by quenching is arbitrary to some extent. It is obvious that the quality of the resulting structure depends on the cooling rate. If the cooling rate is too high the samples will contain more disorder than the real structures, i.e. there is a larger variation in the bond length or bond angles and an excess of free energy per atom. However if the cooling rate is too slow parts of the structure could start to crystallize. It is therefore useful to compare parameters such as coordination numbers, bond deviations and angle deviations to the experimental values measured by x-ray of neutron diffraction. Another parameter indicating the quality of the structure is the number of defects. A device quality semiconductor typically has a defect concentration of 10^{17} cm^{-3} [32]. This implies that a supercell containing 10^6 atoms should have one defect. Smaller supercells should be essentially defect free. Table VI summarizes the number of defects for different cooling rates taking into account the directionality of the bonds. The total amount of defects present

in the fast and normal quench sample is considerably higher than in the slow quench samples. The defects are mostly 3-fold coordinated Si atoms and under/over-coordinated N atoms. The number of “square structures” seems to be unaffected by the different cooling rates. The effect of the cooling rate is also visible in the partial radial distributions (see Figs. 2, 3). The intensity of the first peak in g_{Si-Si} is higher in the fast quench sample. This can be attributed to the higher amount of Si-Si bonds in the structure. The number of Si-H bonds increases with slower cooling as can be seen from the g_{Si-H} function. The increase can be coupled to the number of hydrogen that is incorporated in the amorphous network made up by silicon and nitrogen atoms. It seems that the fast cooling rate produces an excess of H₂ molecules and thus less hydrogen atoms are being incorporated into the network. On the contrary the Si-N and H-N radial distributions are only very slightly affected by the cooling rate.

VII. CONCLUSIONS

We have obtained structural models of a-SiN_x:H using a cooling from a liquid approach. The amorphous network is characterized in terms of partial radial and bond angle distributions. These functions are a prediction, since to our knowledge no scattering data on this particular composition exist. We conclude that a-Si_{0.34}N_{0.35}H_{0.31} can be viewed as a heavily distorted network of c-Si₃N₄ (either α or β phase) interpenetrated with “square structures”. The amount of distortion can be estimated from the deviation of the bond lengths and bond angles (see Tab. I). The “square structure” is a planar configuration of two silicon atoms in opposite corners of a square and two nitrogen atoms in the remaining corners. It is shown that identifying bonded atoms solely on the basis of their distance is not sufficient. The slow quench samples contain a small number of under/over-coordinated atoms. These structural defects can be coupled to electronic defect states in the gap in most of the cases. The electronic defects are identified by evaluating their level of localization. Si-Si bonds give rise to states near both sides of the band gap. This finding is in agreement with the fact that the band gap of a-SiN_x:H increases with increasing nitrogen content. The average band gap value is found to be 2.42 eV with a variation of 0.14 eV.

We examined the effect of the cooling rate on the quality of the amorphous structure. The small number of defects in the slow quench samples gives us confidence that these samples present realistic models of a-SiN_x:H. Note that sample B does not contain any structural nor electronic defects.

ACKNOWLEDGMENT

This work was carried out with a subsidy of the Dutch Ministry of Economic Affairs under EOS-LT program (project number EOSLT02028) and is a part of the research programme of the Stichting voor Fundamenteel Onderzoek der Materie (FOM). FOM is financially supported by the Nederlandse Organisatie voor Wetenschappelijk Onderzoek (NWO).

REFERENCES

- [1] S. L. Luxembourg, P. Kús, and M. Zeman, "Bandgap engineering using a-si:h/a-sin_x:h superlattices," *Annual Workshop on Semiconductor Advances for Future Electronics and Sensors*, vol. 10, 2007.
- [2] F. H. P. M. Habraken and A. E. T. Kuiper, "Silicon nitride and oxynitride films," *Materials Science and Engineering*, vol. R12, pp. 123–175, 1994.
- [3] C. E. Morosanu, "The preparation, characterization and application of silicon nitride thin films," *Thin Solid Films*, vol. 65, pp. 171–208, 1980.
- [4] P. Vashishta, R. K. Kalia, and I. Ebbsjö, "Low-energy floppy modes in high-temperature ceramics," *Phys. Rev. Lett.*, vol. 75, no. 5, pp. 858–861, 1995.
- [5] N. Umetsaki, N. Hirotsuki, and K. Hirao, "Structural characterization of amorphous silicon nitride by molecular dynamics simulation," *Journal of Non-Crystalline Solids*, vol. 150, pp. 120–125, 1992.
- [6] F. de Brito Mota, J. F. Justo, and A. Fazzio, "Structural properties of amorphous silicon nitride," *Phys. Rev. B*, vol. 58, no. 13, pp. 8323–8328, 1998.
- [7] —, "Structural and electronic properties of silicon nitride materials," *Journal of Quantum Chemistry*, vol. 70, pp. 973–980, 1998.
- [8] K. Matsunaga and Y. Iwamoto, "Molecular dynamics study of atomic structure and diffusion behavior in amorphous silicon nitride containing boron," *J. Am. Ceram. Soc.*, vol. 84, pp. 2213–2219, 2001.
- [9] J. F. Justo, F. de Brito Mota, and A. Fazzio, "First-principles investigation of a-sin_x:h," *Phys. Rev. B*, vol. 65, p. 073202, 2002.
- [10] P. Ordejon and F. Yndurain, "Theoretical study of a-sin_xh_y alloys," *Journal of Non-Crystalline Solids*, vol. 137–138, pp. 891–894, 1991.
- [11] F. Alvarez and A. A. Valladares, "Atomic topology and radial distribution functions of a-sin_x alloys: ab initio simulations," *Solid State Communications*, vol. 127, pp. 483–487, 2003.
- [12] R. K. Kalia, A. Nakano, A. Omeltchenko, K. Tsuruta, and P. Vashishta, "Role of ultrafine microstructures in dynamic fracture in nanophase silicon nitride," *Phys. Rev. Lett.*, vol. 78, no. 11, pp. 2144–2147, 1997.
- [13] R. K. Kalia, A. Nakano, K. Tsuruta, and P. Vashishta, "Morphology of pores and interfaces and mechanical behavior of nanocluster-assembled silicon nitride ceramic," *Phys. Rev. Lett.*, vol. 78, no. 4, pp. 689–692, 1997.
- [14] K. Tsuruta, A. Omeltchenko, R. K. Kalia, and P. Vashishta, "Early stage of sintering of silicon nitride nanoclusters: a molecular-dynamics study on parallel machines," *Europhysics Letters*, vol. 33, no. 6, pp. 441–446, 1996.
- [15] K. Tsuruta, A. Nakano, R. K. Kalia, and P. Vashishta, "Dynamics of consolidation and crack growth in nanocluster-assembled amorphous silicon nitride," *J. Am. Ceram. Soc.*, vol. 81, no. 2, pp. 433–436, 1998.
- [16] P. Kroll, "Structure and reactivity of amorphous silicon nitride investigated with density-functional methods," *Journal of Non-Crystalline Solids*, vol. 293–295, pp. 238–243, 2001.
- [17] F. Wooten and D. Weaire, "Generation of random network models with periodic boundary conditions," *J. of Non-Cryst. Solids*, vol. 64, pp. 325–334, 1984.
- [18] S.-Y. Lin, "Hydrogen-induced electronic states and vibrational modes in hydrogenated amorphous silicon nitride," *Thin Solid Films*, vol. 395, pp. 101–104, 2001.
- [19] —, "Electronic and vibrational properties of hydrogenated amorphous silicon nitride," *Journal of Optoelectronics and Advanced Materials*, vol. 4, no. 3, pp. 543–552, 2002.
- [20] —, "Electronic defect states of amorphous silicon nitride," *Optical Materials*, vol. 23, pp. 93–98, 2003.
- [21] L. Martín-Moreno, E. Martínez, J. A. Vergés, and F. Yndurain, "Electronic structure, defect states, and optical absorption of amorphous si_{1-x}n_x [0 ≤ x/(1-x) ≤ 2]," *Phys. Rev. B*, vol. 35, no. 18, pp. 9683–9692, 1987.
- [22] E. San-Fabián, E. Louis, L. Martín-Moreno, and J. A. Vergés, "Possibility of finding reliable solid-state tight-binding parameters for the si-n bond through quantum-chemistry calculations," *Phys. Rev. B*, vol. 39, no. 3, pp. 1844–1855, 1989.
- [23] J. P. Xanthakis, S. Papadopoulos, and P. R. Mason, "The electronic structure of sin_x: the valence band dos and band gaps," *J. Phys. C: Solid State Phys.*, vol. 21, pp. 555–560, 1988.
- [24] J. P. Perdew, J. A. Chevary, S. H. Vosko, K. A. Jackson, M. R. Pederson, D. J. Singh, and C. Fiolhais, "Atoms, molecules, solids, and surfaces: Applications of the generalized gradient approximation for exchange and correlation," *Physical Review B*, vol. 46, no. 11, pp. 6671–6687, 1992.
- [25] G. Kresse and J. Hafner, "Ab initio molecular dynamics for liquid metals," *Phys. Rev. B*, vol. 47, no. 1, pp. 558–561, 1993.
- [26] G. Kresse and J. Furthmüller, "Efficient iterative schemes for ab initio total-energy calculations using a plane-wave basis set," *Phys. Rev. B*, vol. 54, no. 16, pp. 11 169–11 186, 1996.
- [27] P. E. Blöchl, "Projector augmented-wave method," *Phys. Rev. B*, vol. 50, no. 24, pp. 17953–17 979, 1994.
- [28] G. Kresse and D. Joubert, "From ultrasoft pseudopotentials to the projector augmented-wave method," *Phys. Rev. B*, vol. 59, no. 3, pp. 1758–1775, 1999.
- [29] M. Methfessel and A. T. Paxton, "High-precision sampling for brillouin-zone integration in metals," *Phys. Rev. B*, vol. 40, no. 6, pp. 3616–3621, 1989.
- [30] H. J. Monkhorst and J. D. Pack, "Special points for brillouin-zone integrations," *Physical Review B*, vol. 13, no. 12, pp. 5188–5192, 1976.
- [31] G. Kresse and J. Hafner, "Ab initio simulation of the metal/nonmetal transition in expanded fluid mercury," *Phys. Rev. B*, vol. 55, no. 12, p. 7539, 1997.
- [32] R. E. I. Schropp and M. Zeman, *Amorphous and Microcrystalline Silicon Solar Cells: Modelling, Materials and Device Technology*. Kluwer Academic Publishers, 1998.